

“ScatSpotter” 2024 — A Distributed Dog Poop Detection Dataset

Jonathan Crall
Kitware

jon.crall@kitware.com

Abstract

We introduce a new — currently 42 gigabyte — “living” dataset of phone images of dog feces, annotated with manually drawn or AI-assisted polygon labels. There are 6k full resolution images and 4k detailed polygon annotations. The collection and annotation of images started in late 2020 and the dataset grows by roughly 1GB a month.

We train VIT and MaskRCNN baseline models to explore the difficulty of the dataset. The best model achieves a pixel-wise average precision of 0.858 on a 691-image validation set and 0.847 on a small independently captured 30-image contributor test set.

The most recent snapshot of dataset is made publicly available through three different distribution methods: one centralized (Girder) and two decentralized (IPFS and BitTorrent). We study of the trade-offs between distribution methods and discuss the feasibility of each with respect to reliably sharing open scientific data.

The code to reproduce the experiments is hosted on GitHub, and the data is published under the Creative Commons Attribution 4.0 International license. Model weights are made publicly available with the dataset. Experimental hardware, time, energy, and emissions are quantified.

1. Introduction

Applications for a computer vision system capable of detecting and localizing poop in images are numerous. These include automated waste disposal to keep parks and backyards clean, tools for monitoring wildlife populations via droppings, and a warning system in smart-glasses to prevent people from stepping in poop. Our primary motivating use case is a phone application that assists dog owners in locating their dog’s poop in a leafy park for easier cleanup. Many of these applications can be realized with modern object detection and segmentation methods [45, 47, 51] combined with a large labeled dataset.

In addition to enabling several applications, poop detection is an interesting benchmark problem. It is relatively simple, with a narrow focus on a single class, making it suit-



Figure 1. A zoomed in example of an annotated object in a challenging condition: a scene cluttered with leaves. The similarity between the leaves and the poop causes a camouflage effect that can make detecting it difficult.



Figure 2. The “before/after/negative” protocol. The orange box highlights the location of the poop in the “before” image. In the “after” image, it is the same scene but the poop has been removed. The “negative” image is a nearby similar scene, potentially with a distractor. Note that the object is small relative to the image size.

able for exploring the capabilities of object detection models that target a single labeled class. However, the task includes non-trivial challenges such as resolution issues (e.g., camera quality, distance), camouflaging distractors (e.g., leaves, pine cones, sticks, dirt, and mud), occlusion (e.g., bushes, overgrown grass), and variation in appearance (e.g., old vs. new, healthy vs. sick). An example of a challenging case is shown in Fig. 1. Investigation into cases where this problem is difficult may provide insight into how to better train object

Name	# Cats	# Images	# Annots	Image W × H	Annot Area ^{0.5}	Size	Annot Type
ImageNet LSVRC2017 [44]	1,000	594,546	695,776	500 × 374	239	166GB	box
MSCOCO 2017 [30]	80	123,287	896,782	428 × 640	57	50GB	polygon
CityScapes [11]	40	5,000	287,465	2,048 × 1,024	50	78GB	polygon
ZeroWaste [3]	4	4,503	26,766	1,920 × 1,080	200	10GB	polygon
TrashCanV1 [22]	22	7,212	12,128	480 × 270	54	0.61GB	polygon
UAVWaste [27]	1	772	3,718	3,840 × 2,160	55	2.9GB	polygon
SpotGarbage-GINI [37]	1	2,512	337	754 × 754	355	1.5GB	classification
TACO [42]	60	1,500	4,784	2,448 × 3,264	119	17GB	polygon
MSHIT [35]	2	769	2,348	960 × 540	99	4GB	box
“ScatSpotter” (ours)	1	6,648	4,386	4,032 × 3,024	96	42GB	polygon

Table 1. Related Datasets. The first 4 columns provide the name of the dataset, the number of categories, images, and annotations. Image W × H is the pixel width and height of the image with the median area. Annot Area^{0.5} is the median sqrt(area) in pixels of the annotation polygon or box. The Size column refers to the size of the dataset in gigabytes. Annot Type refers to if the dataset is annotated with bounding boxes, image-level classification labels, or polygon segmentations. Figure 3 provides a visual gist of the distribution of annotation shape, size, and positional in each dataset.

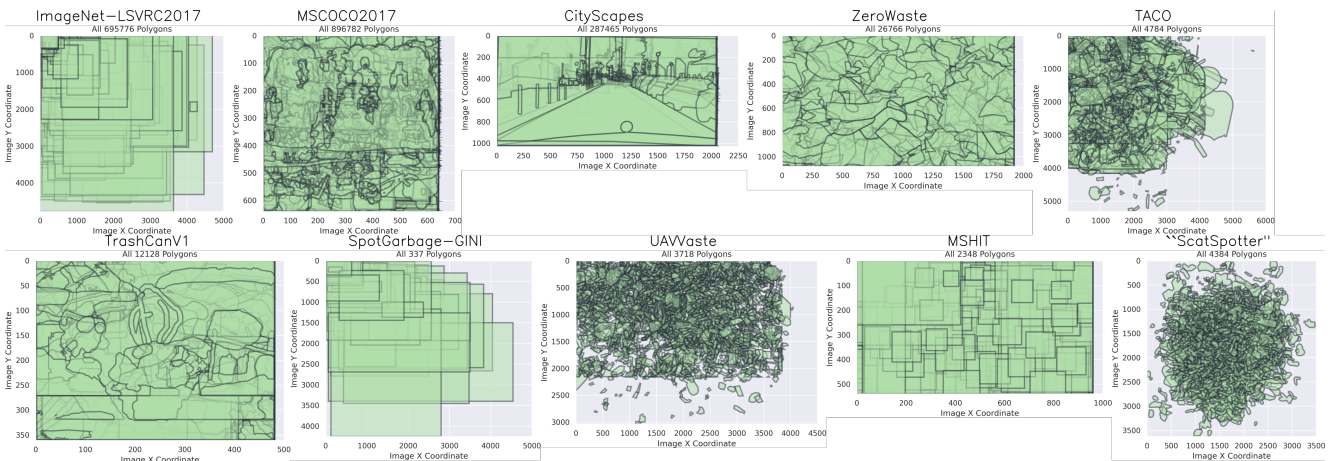


Figure 3. A comparison of all of the annotations for different datasets including ours. All polygon annotations drawn in a single plot with 0.8 opacity to demonstrate the distribution in annotation location, shape, and size with respect to image coordinates.

detection and segmentation networks.

Towards these ends we introduce a new dataset, which in formal settings, we call “ScatSpotter”. Poops are annotated with polygons making the dataset suitable for training detection and segmentation models. In order to assist with annotation and add variation, we collect images using a “before/after/negative” protocol as shown in Figure 2.

From this data, we train a segmentation model to classify which pixels in an image contain poop and which do not. Our models show strong performance, but there are notable failure cases indicating this problem is difficult even for modern computer vision algorithms.

To enable others to build on our results, it is essential that the dataset is accessible and hosted reliably. Centralized methods are a typical choice, offering high speeds, but they can be costly for individuals, often requiring institutional

support or paid hosting services. They are also prone to outages and lack built-in data validation. In contrast, decentralized methods allow volunteers to host data and offers built-in validation of data integrity. This motivates us to compare and contrast the decentralized BitTorrent [7], and IPFS [4] protocols as mechanisms for distributing datasets.

Our contributions are: 1) A challenging new **open dataset** of images with polygon annotations. 2) A set of trained **baseline models**. 3) An observational **comparison of dataset distribution methods**.

2. Related Work

To the best of our knowledge, our dataset is currently the largest publicly available collection of annotated dog poop images, but it is not the first. A dataset of 100 dog poop images was collected and used to train a FasterRCNN model

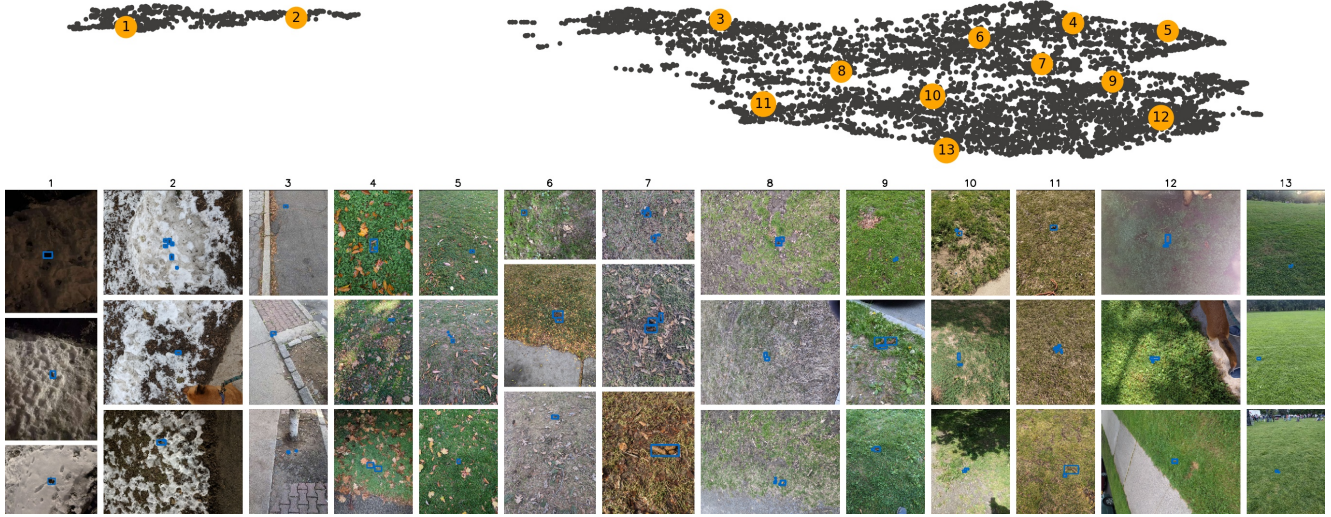


Figure 4. Example images from the dataset based on 2D UMAP [34] clusters over the dataset. Each point in the top image is a 2D-projected image embedding. Each numbered orange dot corresponds to three nearby images, which are drawn in columns on the bottom. Annotation boxes are drawn in blue. An interesting observation is that there is a clear separation into two UMAP blobs represents snowy versus (columns 1 and 2) non-snowy images (columns 3-13). We verified that this pattern holds beyond the examples explicitly shown here.

[39] but this dataset and model are not publicly available. The company iRobot has a dataset of annotated indoor poop images used to train Roomba j7+ to avoid collisions [19], but as far as we are aware, this is not available. In terms of available poop detection datasets we are only aware of MSHIT [35] which is much smaller, only contains box annotations, and the objects of interest are plastic toy poops.

Compared to benchmark object localization and segmentation datasets [11, 30, 44] ours is much smaller and focused only on a single category. However, when compared to litter and trash datasets [3, 22, 27, 37, 42] ours is among the largest in terms of number of images / annotations, image size, and total dataset size. ZeroWaste [3] uses a “before/after” protocol similar to our BAN-protocol. We provide an overview of these related datasets in Table 1. Among all of these, ours stands out for having the highest resolution images and the smallest objects relative to that resolution. For a review of additional waste related datasets, refer to [36].

Section 5 discusses the logistics and tradeoffs between dataset distribution mechanisms with a focus on comparing centralized and decentralized methods. IPFS [7] and BitTorrent [4] are the decentralized mechanisms we evaluate, but others exist such as Secure Scuttlebut [49] and Hypercore [16], which we did not test.

3. Dataset

Our first contribution is the creation of a new open dataset which consists of images of dog poop in mostly urban, mostly outdoor environments. The data is annotated to support object detection and segmentation tasks. The majority

of the images feature fresh poop from three specific dogs, but there are a significant number of images with poops of unknown age and from unknown dogs.

To provide a gist of the image variations in the dataset we computed UMAP [34] image embeddings based on ResNet50 [21] descriptors display images corresponding with clusters in this embedding in Figure 4.

More details about the dataset are available in a standardized datasheet [17] that covers the motivation, composition, collection, preprocessing, uses, distribution, and maintenance. This will be distributed with the data itself, and is provided in supplemental material.

3.1. Dataset Collection

The dataset was primarily collected by a single researcher while walking their dogs. When they encountered a poop in public areas — usually freshly created by one of their own dogs, but sometimes from other dogs — they would take an image of the poop from their original vantage point. Occasionally, they would move closer or further away to add variation to the dataset. After taking a photo, they would pick it up and dispose of it.

Most images in the dataset follow a “before/after/negative” (B/A/N) protocol. The first image is the “before” picture of the poop. After picking up the poop, an “after” picture of the same area was taken from approximately the same angle and distance. Finally, a “negative” image was captured of a nearby area or object that might be confused with dog poop (e.g., pine cones, leaves, sticks, dark areas on snow). While we only use these B/A/N triples to sample negative regions, they may be useful for constructing contrastive triplet-style

losses [46].

The majority of images follow the triple-pattern protocol. However, there are exceptions. The first six months of data collection only involved the “before/after” part of the protocol, and we began collecting the third negative image after a colleague suggested it. In some cases, the researcher failed or was unable to take the second or third image. These exceptions were programmatically identified.

In addition to the primary dataset, we also received 84 images from contributors. Most of these images do not follow the B/A/N protocol, are only used in testing, and are *not* included in the following analysis.

3.2. Dataset Annotation

Originally the “before” and “after” images were meant to help with automatic annotation, but this idea was not successful due to unreliable image-alignment. However, with the Segment Anything Model (SAM) [25] model, we were able to efficiently annotation the dataset.

Specifically, images were annotated using labelme [24]. Most annotations were initialized using SAM and a point prompt. All AI polygons were manually reviewed. In most cases only small manual adjustments were needed, but there were a significant number of cases where SAM did not work well and fully manual annotations were needed. Regions with shadows seemed to cause SAM the most trouble, but there were other failure cases. Unfortunately, there is no metadata to indicate which polygons were manually created or done using AI. However, the number of vertices may be a reasonable proxy to estimate this, as polygons generated by SAM tend to have higher fidelity boundaries. The boundaries of 4,386 annotated polygons are illustrated in Figure 3.

3.3. Dataset Stats and Analysis

As of 2024-07-03, the primary dataset consists of 6,648 images and 4,386 annotations, spanning 3.5 years. The data was captured at a relatively uniform rate over this period, primarily in parks and sidewalks within a small city. Weather conditions varied across snowy, sunny, rainy, and foggy. A visual representation of the distribution of seasons, time-of-day, daylight, and capture rate is provided in Figure 5.

The dataset images are available in full resolution, without any resampling or resizing. Almost all images were taken using the same phone-camera, with a consistent width/height ratio of $4,032 \times 3,024$ (although some may be rotated based on EXIF data). Six images have a slightly different resolution of $4,008 \times 5,344$, and one has a resolution of $7,680 \times 1,024$. The images are stored as 8-bit JPEGs with RGB channels, and most include overviews (i.e., image pyramids), allowing for fast loading of downscaled versions.

Due to the “B/A/N” protocol, approximately one-third of the dataset contains annotations, as the other two-thirds of images were taken after removing the object of interest

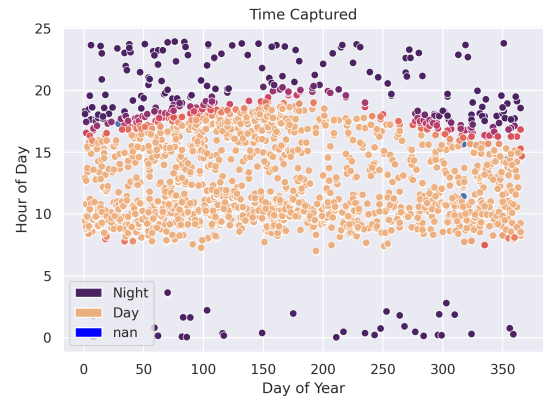


Figure 5. Scatterplot of the time-of-year vs time-of-day each image was taken. On the x-axis, 0 is January 1st. On the y-axis, 0 is midnight. For images with geolocation and timestamp (assuming the timezone is local or given and correct) we also estimate the amount of daylight as indicated by the color of each dot. While the majority of the images are taken in daylight, there are a sizable number of nighttime images taken with longer exposure, flash on, or sometimes flash off in streetlights.

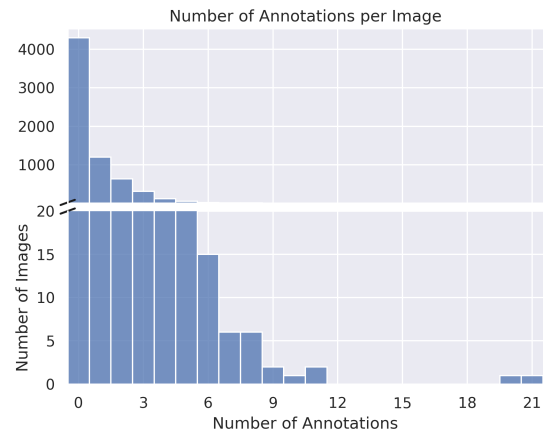


Figure 6. Histogram of the number of annotations per image. Only 35% (2,346) of the images contain annotations, the other 65% (4,302) are known not to contain poop. Of these about half of them were taken directly after the poop was picked up. The other half are pictures of a nearby location.

from the scene. Consequently, most images have no annotations. The next most frequent number of annotations is one, but images can contain multiple annotations due to several reasons: 1) A single poop may break into multiple disjoint parts (although the exact criteria for this can be ambiguous). 2) Two dogs may have pooped nearby each other. 3) One or more dogs may have pooped in the same area over a period of time (in some cases, it can be challenging to determine if it is poop or dirt). The number of annotations per image is illustrated in Figure 6.

3.4. Dataset Splits

Our dataset is split into training, validation, and test sets based on the year and day of image capture. Specifically, images from 2021, 2022, and 2023 are assigned to the training set, while images from 2020 are used for validation. For data from 2024, we consider the Gregorian ordinal date n of each image and include it in the validation set if $n \equiv 0 \pmod{3}$; otherwise, it is assigned to the training set.

The resulting splits are as follows: Our training dataset consists of 5,747 images and is identified by a suffix of `1e73d54f`, which is the prefix of a hash of its contents. The validation set contains 691 images and has a suffix of `99b22ad0`. The test set, consisting of the 30 contributor images with at least one annotation, has a suffix of `d8988f8c`. These splits are provided in the COCO JSON format [30].

4. Baseline Models

As our second contribution, we trained and evaluated models to establish a baseline for future comparisons. Specifically we train three model variants. We trained two MaskRCNN [20] models (specifically the `R_50_FPN_3x` configuration), one starting from pretrained ImageNet weights (MaskRCNN-pretrained), and one starting from scratch (MaskRCNN-scratch). We also trained a semantic segmentation vision transformer (ViT-sseg-scratch) [12, 18], which was only trained from scratch.

We performed two types of evaluations on the models. “Box” evaluation computes standard COCO object detection metrics [30]. MaskRCNN natively outputs scored bounding boxes, but for the ViT-sseg model, we convert heatmaps into boxes by thresholding the probability maps and converting taking the extend of the resulting polygons as bounding boxes. The score is taken as the average heatmap response under the polygon. Bounding box evaluation has the advantage that small and large annotations contribute equally to the score, but it can also be misleading for datasets where the notion of an object instance can be ambiguous.

To complement the box evaluation, we performed a pixelwise evaluation, which is more sensitive to the details of the segmented masks, but also can be biased towards larger annotations with more pixels. The corresponding truth and predicted pixels were accumulated into a confusion matrix, allowing us to compute standard metrics such as precision, recall, false positive rate, etc... [41]. For the ViT-sseg model, computing this score is straightforward, but for MaskRCNN we accumulate per-box heatmaps into a larger full image heatmap, which can then be scored.

Quantitative results for each of these models on box and pixel metrics are shown in Table 2. Because the independent test set is only 30 images, we also present results on the larger validation dataset. Note that the evaluated models were selected based on their validation scores. Correspond-

ing qualitative results are illustrated in Figure 7 for the test dataset and Fig. 8 for the validation dataset.

All models were trained on a single machine with an Intel Core i9-11900K CPU and an NVIDIA GeForce RTX 3090 GPU. The total time spent on prediction and evaluation across all experiments was 15.6 days, with prediction consuming 109.6.3 kWh of electricity and causing an estimated emissions of 23.0 CO₂kg as measured by CodeCarbon [28].

We estimated train-time resource usage during training using indirect methods, assuming a constant power draw of 345W from the RTX 3090 GPU. Electricity consumption was approximated accordingly, while emissions were calculated using a conversion ratio of $0.21 \frac{\text{kgCO}_2}{\text{kWh}}$ derived from our prediction time measurements. Based on file timestamps, we estimated that running 44 different training runs took approximately 159.66 days, resulting in an estimated electricity usage and emissions of 1321.99 kWh and 277.612 CO₂ kg, respectively.

A key limitation of these results is the imbalance between model types, with 42 out of 44 trained models being ViT-ssegs and only two MaskRCNN models, each taking approximately 8 hours to train. More details on the ViT-sseg experiments can be found in the supplemental materials.

5. Open Data Distribution

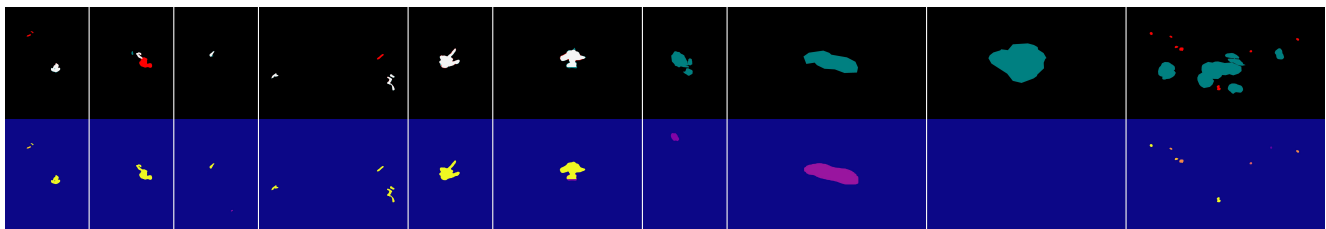
Empirical evidence suggests that a substantial proportion of scientific studies have low reproducibility rates, which has raised concerns across various disciplines [2]. Ideally, all scientific research should be independently reproducible. Despite higher success rates in computer science (up to 60%) compared to other fields, there is still room for improvement [10, 13, 43]. Addressing this issue requires not just better experimental documentation but also more reliable and accessible data distribution methods. Specifically, this involves robustly codifying data download and preparation processes.

Centralized data distribution methods allow for codified data access by storing URLs that point to datasets within the code, offering fast and direct access. However, this approach lacks robustness. It can fail if the provider goes offline, changes the URL, or stops hosting the data. Additionally, cloud storage can be expensive, and users must trust that the provider delivers the correct data — a risk that can be mitigated by using checksums to verify data integrity.

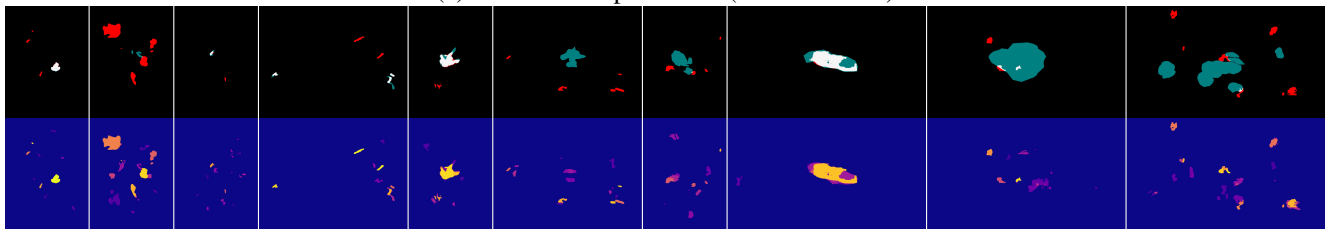
In contrast, decentralized methods allow users to access data in the same way, even if the organization hosting the data changes. By leveraging content-addressable storage, where the dataset checksum acts as both the key to locate and validate the data, these methods ensure data integrity and nearly eliminate the risk of dead URLs, provided that at least one peer retains the data. While decentralized systems face challenges such as longer connection times, increased network overhead, and the need for a robust peer network, their ability to ensure data accessibility via a static address

Dataset split:		Test				Validation			
Evaluation type:		Box		Pixel		Box		Pixel	
Model type	# Params	AP	AUC	AP	AUC	AP	AUC	AP	AUC
MaskRCNN-pretrained	43.9e6	0.661	0.692	0.847	0.858	0.612	0.721	0.858	0.905
MaskRCNN-scratch	43.9e6	0.384	0.573	0.581	0.804	0.255	0.576	0.434	0.891
VIT-sseg-scratch	25.5e6	0.520	0.522	0.505	0.913	0.476	0.532	0.780	0.994

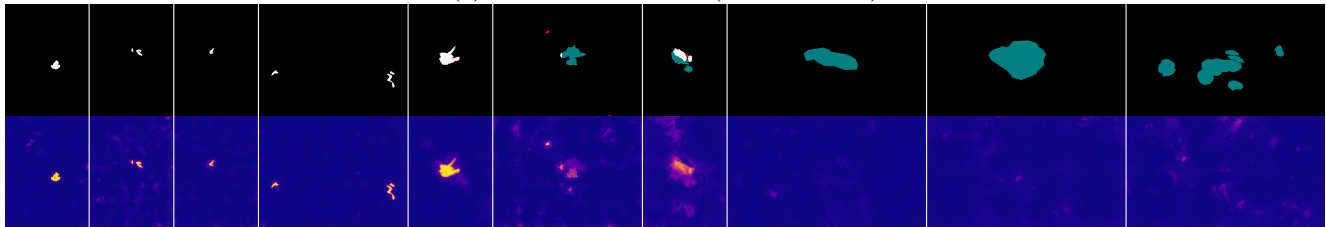
Table 2. Quantitative results on the test and validation datasets. Unsurprisingly, the model starting with pretrained weights scores best. Models are evaluated using bounding-box metrics (under the Box column) as well as pixelwise-segmentation metrics (under the Pixel column). We consider positive predictive value (ppv or precision), true-positive-rate (tpr or recall), and false positive rate (fpr). The average precision (AP) is the area under the ppv/tpr curve [41]. The AUC is the area under the tpr/fpr curve. Thus AP is more sensitive to ppv and AUC is more sensitive to fpr. All metrics were computed using scikit-learn [40]. We note an important limitation of our results: much more time was spent tuning the VIT-sseg model. It is likely that MaskRCNN results could be improved with further tuning.



(a) MaskRCNN-pretrained (test set results)



(b) MaskRCNN-scratch (test set results)



(c) VIT-sseg-scratch (test set results)



(d) Input images from the 30-image test set

Figure 7. Qualitative results using the top-performing model on the validation set, applied to a selection of images from the test set. Subfigure (d) shows the input image for the above predictions. In the first three subfigures (a, b, and c), the top row is a binarized classification map, where true positive pixels are shown in white, false positives in red, false negatives in teal, and true negatives in black. The second row in each subfigure is the predicted heatmap, illustrating the model’s output before binarization. The threshold for binarization was set to 0.5 in all cases. All three methods show clear responses to objects of interest, but cases where objects are close-up and partially deteriorated do seem to be a common failure mode. Camouflage is likely a failure case, but this dataset does not contain many examples.

motivates our investigation

Specifically, we focus on two prominent candidates: Bit-

Torrent and IPFS. BitTorrent [7, 8] is a well known sharing protocol that originally relied on centralized trackers and

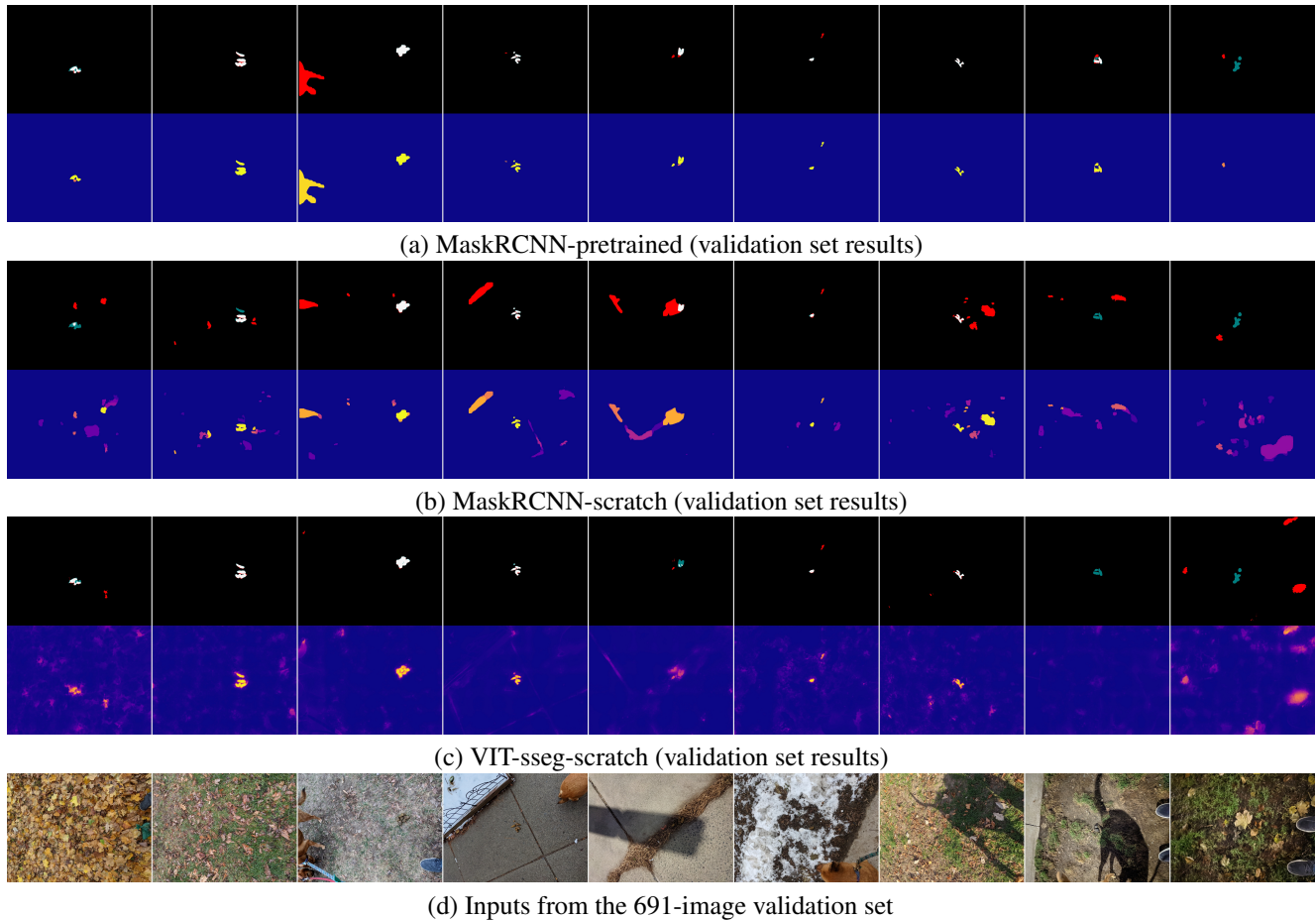


Figure 8. Qualitative results using the top-performing model on the validation set, applied to a selection of images from the validation set. See Figure 7 for an explanation of the visualizations. Each model was selected based on its performance on this dataset, which may cause spurious cases that agree with the truth labels, but this dataset was never used to compute a gradient, which still make these valuable results for assessing generalizability. Notably the models were able to pick out camouflaged cases on the left, but not all on the right.

databases of torrent files to connect peers. While trackers and torrent files are still prominent, torrents can be published to a distributed hash table (DHT) using the Kademlia algorithm [33]. This makes it a strong candidate for a decentralized distribution mechanism. On the other hand, IPFS (InterPlanetary File System) [4, 6] is a newer tool directly build directly on a DHT. IPFS has been likened to “a single BitTorrent swarm, exchanging objects within one Git repository”. Both IPFS and BitTorrent are content addressable at the dataset level, which makes them both appropriate for our use case where we seek a static address that can be used to robustly access data.

The specific 2024-07-03 version of the dataset used in this paper has the IPFS CID (content identifier) of: `bafybeiedwp2zvmadyb2c2axrcl455xfbv2mgdbhgkc3dile4dftiimwth2y`. The torrent has a magnet URL of: `magnet:?xt=urn:btih:ee8d2c87a39ea9bfe48bef7eb4ca12eb68852c49`, and is tracked on

Academic Torrents [9].

For practitioners, the key practical concern is how quickly and reliably data can be accessed. By comparing IPFS, BitTorrent, and centralized mechanisms access times for our dataset, we aim to make explicit the tradeoffs between the methods to help others make an informed choice about adopting decentralized methods.

5.1. Distribution Observational Study

Our third contribution is an observational study of decentralized and centralized data distribution methods. For centralized distribution, we use a self-hosted instance of Girder [38]. For decentralized clients, we use Transmission [29] (BitTorrent) and Kubo [23] (IPFS). As a baseline, we also measure direct transfers using Rsync[50].

To assess the effectiveness of each mechanism we programmatically download our 42GB dataset and measure the time required to complete the transfer. Each experiment was

method	num	mean	std	min	max
BitTorrent	5	8.36h	5.16h	2.21h	14.39h
IPFS	5	10.68h	9.54h	1.80h	24.62h
Girder	5	2.85h	2.31h	1.05h	6.24h
Rsync	5	4.84h	1.39h	3.10h	6.10h

Table 3. Transfer times (in hours) for our 42GB dataset, averaged over multiple trials (indicated in the “num” column). Girder and Rsync, tend to exhibit faster less varied transfer times compared to the IPFS and BitTorrent when few seeders are available.

run multiple times, machines were separated by approximately 30 kilometers with an average ping time of 48.48 ms. For each test, we log transfer start and end times along with notes and code (provided in supplemental materials).

While our measurements provide a reasonable estimate of for access time for each mechanism, there are notable limitations in our methodology. First, different machines and networks have different upload and download speeds, and network congestion is variable. For decentralized methods, we lack an automated mechanism separate peer-connection time and actual download time. Additionally, Girder required data to be packed into archive files, improving transfer efficiency due to fewer file boundaries. In all other methods, we provide granular access to each file in the dataset, which avoids an extra unpacking step and enables sharing of the same file between different versions of the datasets, but decreases transfer efficiency. Another confounding factor is that with decentralized mechanisms the number of seeders is not controlled for. Subsets of the data have been hosted on IPFS for years, and portions of the dataset may be provided by unknown members of the network. For BitTorrent, our initial transfers only had one seeder, but during our tests other nodes accessed and started to provide the data.

With these limitations acknowledged, we present the transfer times statistics in Table 3. Alongside these measurements, several anecdotal observations are worth noting. Transferring files using IPFS involved prohibitively expensive peer discovery times, and we were only able to connect two machines after manually informing them of each other’s peer ID. For BitTorrent, were unable to use the mainline DHT and fell back to using trackers. We believe these peer discovery issues are because the dataset has a small number of seeders. To test this, we downloaded other established datasets via IPFS and BitTorrent and found that the peer discovery time was almost immediate, suggesting that this becomes less of an issue as a dataset is shared. However, the inability to quickly find a single nearby peer with the data is a major issue for initial or private dataset development.

Despite significant testing limitations, our measurements quantify the expected data-access time penalty to gain the

advantages of decentralized mechanisms. The minimum time column shows that each method can be competitive, but on average decentralized mechanisms are significantly slower and can be stifled by long peer-discovery times.

6. Conclusion

We have introduced the largest open dataset of high resolution images with polygon segmentations of dog poop, collected with a “before/after/negative” (BAN) protocol. The dataset contains several challenges including amorphous objects, multi-season variation, difficult distractors, daytime / nighttime variation. We have described the dataset collection and annotation process and reported statistics on the dataset.

We provided a recommended train/validation/test split of the dataset, and used this to train and evaluate several baseline segmentation models. In addition to providing quantitative and qualitative results of the models, we also report the resources required to perform these training, prediction, and evaluation experiments.

We have published our data and models under a permissive license, and made them available through both centralized (Girder) and decentralized (BitTorrent and IPFS) mechanisms. Our evaluation of these distribution methods revealed that while decentralized approaches offer strong data integrity guarantees and content addressable storage that is resistant to dead URLs, data access time can be slower compared to centralized ones, they are often hindered by long peer discovery times when few seeders are available.

Looking towards the future, our planned directions for research and development are: 1) Training a model optimized for mobile devices. 2) Mine hard negatives based on false positives in the training set. 3) Build and publish a phone application that uses the mobile-optimized model to detect poop in real time. 4) Collect more data.

We envision exciting possibilities for the BAN protocol in computer vision research. We hope our work will inspire others to adopt decentralized content addressable data sharing, fostering open collaboration and reproducible experiments. Furthermore, we encourage the community to track experimental resource usage to better understand and offset our experiments’ environmental impact. Moreover, we aspire for our dataset to enable the creation of poop-aware applications. Ultimately, our goal is for this research to contribute meaningfully to the advancement of computer vision and have a positive impact on society.

7. Acknowledgements

We would would like to thank all of the dogs that produced subject matter for the dataset, all of the contributors for helping to construct a challenging test set, and Anthony Hoogs for several suggestions including taking the third negative picture.

References

- [1] Jordan T. Ash and Ryan P. Adams. On Warm-Starting Neural Network Training. In *NeurIPS*. Curran Associates, Inc, 2020.
- [2] Monya Baker. 1,500 scientists lift the lid on reproducibility. *Nature*, 533(7604):452–454, 2016.
- [3] Dina Bashkirova, Mohamed Abdelfattah, Ziliang Zhu, James Akl, Fadi Alladkani, Ping Hu, Vitaly Ablavsky, Berk Calli, Sarah Adel Bargal, and Kate Saenko. ZeroWaste Dataset: Towards Deformable Object Segmentation in Cluttered Scenes. In *CVPR*, pages 21147–21157, 2022.
- [4] Juan Benet. IPFS - Content Addressed, Versioned, P2P File System. *ArXiv*, abs/1407.3561, 2014.
- [5] Gedas Bertasius, Heng Wang, and Lorenzo Torresani. Is space-time attention all you need for video understanding? In *ICML*, page 4, 2021.
- [6] Christian Bieri. An overview into the InterPlanetary File System (IPFS): use cases, advantages, and drawbacks. *Communication Systems XIV*, 28, 2021.
- [7] Bram Cohen. Incentives Build Robustness in BitTorrent. In *Workshop on Economics of Peer-to-Peer systems*, pages 68–72, 2003.
- [8] Bram Cohen. The BitTorrent Protocol Specification v2. https://www.bittorrent.org/beps/bep_0052.html, 2017. Accessed: 2024-08-23.
- [9] Joseph Paul Cohen and Henry Z. Lo. Academic torrents: A community-maintained distributed repository. In *Annual Conference of the Extreme Science and Engineering Discovery Environment*, 2014.
- [10] Christian Collberg and Todd A Proebsting. Repeatability in computer systems research. *Communications of the ACM*, 59(3):62–69, 2016.
- [11] Marius Cordts, Mohamed Omran, Sebastian Ramos, Timo Scharwächter, Markus Enzweiler, Rodrigo Benenson, Uwe Franke, Stefan Roth, and Bernt Schiele. The cityscapes dataset. In *CVPRW*, page 1, 2015.
- [12] Jon Crall, Connor Greenwell, David Joy, Matthew Leotta, Aashish Chaudhary, and Anthony Hoogs. GeoWATCH for Detecting Heavy Construction in Heterogeneous Time Series of Satellite Images. In *IGARSS*, 2024.
- [13] Abhyuday Desai, Mohamed Abdelhamid, and Nakul R. Padalkar. What is Reproducibility in Artificial Intelligence and Machine Learning Research? *ArXiv*, abs/2407.10239, 2024.
- [14] Shibhansh Dohare, J. Fernando Hernandez-Garcia, Parash Rahman, Richard S. Sutton, and A. Rupam Mahmood. Loss of Plasticity in Deep Continual Learning. *ArXiv*, abs/2306.13812, 2023. arXiv:2306.13812 [cs].
- [15] Alexey Dosovitskiy, Lucas Beyer, Alexander Kolesnikov, Dirk Weissenborn, Xiaohua Zhai, Thomas Unterthiner, Mostafa Dehghani, Matthias Minderer, Georg Heigold, Sylvain Gelly, Jakob Uszkoreit, and Neil Houlsby. An Image is Worth 16x16 Words: Transformers for Image Recognition at Scale. *ICLR*, 2021.
- [16] Paul Frazee and Mathias Buss. DEP-0002: Hypercore - Dat Protocol. <https://www.datprotocol.com/deps/0002-hypercore/>. Accessed: 2024-08-23.
- [17] Timnit Gebru, Jamie Morgenstern, Briana Vecchione, Jennifer Wortman Vaughan, Hanna Wallach, Hal Daumé III, and Kate Crawford. Datasheets for datasets. *Communications of the ACM*, 64(12):86–92, 2021.
- [18] Connor Greenwell, Jon Crall, Matthew Purri, Kristin Dana, Nathan Jacobs, Armin Hadzic, Scott Workman, and Matt Leotta. Watch: Wide-area terrestrial change hypercube. In *WACV*, pages 8277–8286, 2024.
- [19] Devindra Hardawar. iRobot’s latest Roomba can detect pet poop (and if it fails, you’ll get a new one). <https://www.engadget.com/irobot-roomba-j-7-object-poop-detection-040152887.html>, 2021. Accessed: 2024-08-23.
- [20] Kaiming He, Georgia Gkioxari, Piotr Dollár, and Ross Girshick. Mask r-cnn. In *ICCV*.
- [21] Kaiming He, Xiangyu Zhang, Shaoqing Ren, and Jian Sun. Deep residual learning for image recognition. In *Proceedings of the IEEE conference on computer vision and pattern recognition*, pages 770–778, 2016.
- [22] Jungseok Hong, Michael Fulton, and Junaed Sattar. Trashcan: A semantically-segmented dataset towards visual detection of marine debris. *ArXiv*, abs/2007.08097, 2020.
- [23] Jeromy Johnson, Juan Benet, Steven Allen, et al. ipfs/kubo. <https://github.com/ipfs/kubo>, 2024. Accessed: 2024-08-23.
- [24] Wada Kentaro. Labelme: Image polygonal annotation with python. <https://github.com/labelmeai/labelme>. Accessed: 2024-08-23.
- [25] Alexander Kirillov, Eric Mintun, Nikhila Ravi, Hanzi Mao, Chloe Rolland, Laura Gustafson, Tete Xiao, Spencer Whitehead, Alexander C. Berg, Wan-Yen Lo, Piotr Dollar, and Ross Girshick. Segment Anything. In *ICCV*, pages 4015–4026, 2023.
- [26] Keith Kirkpatrick. The Carbon Footprint of Artificial Intelligence. *Communications of the ACM*, 66(8):17–19, 2023.
- [27] Marek Kraft, Mateusz Piechocki, Bartosz Ptak, and Krzysztof Walas. Autonomous, onboard vision-based trash and litter detection in low altitude aerial images collected by an unmanned aerial vehicle. *Remote Sensing*, 13(5), 2021.
- [28] Alexandre Lacoste, Alexandra Luccioni, Victor Schmidt, and Thomas Dandres. Quantifying the carbon emissions of machine learning. *ArXiv*, abs/1910.09700, 2019.
- [29] Jordan Lee, Josh Elsasser, Eric Petit, and Mitchell Livingston. Transmission. <https://github.com/transmission/transmission>, 2024. Accessed: 2024-08-23.
- [30] Tsung-Yi Lin, Michael Maire, Serge Belongie, James Hays, Pietro Perona, Deva Ramanan, Piotr Dollár, and C. Lawrence Zitnick. Microsoft COCO: Common Objects in Context. In *Computer Vision – ECCV 2014*, pages 740–755, Cham, 2014. Springer International Publishing.
- [31] Tsung-Yi Lin, Priya Goyal, Ross Girshick, Kaiming He, and Piotr Dollár. Focal loss for dense object detection. In *CVPR*, pages 2980–2988, 2017.
- [32] Ilya Loshchilov and Frank Hutter. Decoupled Weight Decay Regularization. In *ICLR*, 2019.

- [33] Petar Maymounkov and David Mazières. Kademia: A Peer-to-Peer Information System Based on the XOR Metric. In *Peer-to-Peer Systems*, pages 53–65. Springer, Berlin, Heidelberg, 2002.
- [34] Leland McInnes, John Healy, and James Melville. UMAP: Uniform Manifold Approximation and Projection for Dimension Reduction. *ArXiv*, 2020.
- [35] Mikian. Dog Poop (MSHIT). <https://www.kaggle.com/datasets/mikian/dog-poop>, 2020. Accessed: 2024-08-23.
- [36] Agnieszka Mikołajczyk. Waste datasets review. <https://github.com/Agamiko/waste-datasets-review>, 2024. Accessed: 2024-09-07.
- [37] Gaurav Mittal, Kaushal B Yagnik, Mohit Garg, and Narayanan C Krishnan. Spotgarbage: smartphone app to detect garbage using deep learning. In *Proceedings of the 2016 ACM International Joint Conference on Pervasive and Ubiquitous Computing*, pages 940–945, 2016.
- [38] Zack Mullen, Brian Helba, David Manthy, et al. Girder: a data management platform. <https://girder.readthedocs.io/en/latest>, 2024. Accessed: 2024-08-23.
- [39] Neeraj Madan. Dog Poop Detection: Deep Learning (Details). <https://www.youtube.com/watch?v=qGNbHwp0jM8>, 2019. Accessed: 2024-08-23.
- [40] F. Pedregosa, G. Varoquaux, A. Gramfort, V. Michel, B. Thirion, O. Grisel, M. Blondel, P. Prettenhofer, R. Weiss, V. Dubourg, J. Vanderplas, A. Passos, D. Cournapeau, M. Brucher, M. Perrot, and E. Duchesnay. Scikit-learn: Machine learning in Python. *Journal of Machine Learning Research*, 12:2825–2830, 2011.
- [41] David Martin Powers. Evaluation: from precision, recall and F-measure to ROC, informedness, markedness and correlation. *Journal of Machine Learning Technologies*, 2(1):37–63, 2011.
- [42] Pedro F Proença and Pedro Simões. Taco: Trash annotations in context for litter detection. *ArXiv*, abs/2003.06975, 2020.
- [43] Edward Raff. A step toward quantifying independently reproducible machine learning research. In *NeurIPS*. Curran Associates, Inc., 2019.
- [44] Olga Russakovsky, Jia Deng, Hao Su, Jonathan Krause, Sanjeev Satheesh, Sean Ma, Zhiheng Huang, Andrej Karpathy, Aditya Khosla, Michael Bernstein, Alexander C. Berg, and Li Fei-Fei. ImageNet Large Scale Visual Recognition Challenge. *IJCV*, 115(3):211–252, 2015.
- [45] Mark Sandler, Andrew Howard, Menglong Zhu, Andrey Zhmoginov, and Liang-Chieh Chen. MobileNetV2: Inverted Residuals and Linear Bottlenecks. In *CVPR*, pages 4510–4520, 2018.
- [46] Florian Schroff, Dmitry Kalenichenko, and James Philbin. FaceNet: A Unified Embedding for Face Recognition and Clustering. In *CVPR*, pages 815–823, 2015.
- [47] Mennatullah Siam, Mostafa Gamal, Moemen Abdel-Razek, Senthil Yogamani, and Martin Jagersand. RTSeg: Real-Time Semantic Segmentation Comparative Study. In *ICIP*, pages 1603–1607, 2018.
- [48] Leslie N Smith and Nicholay Topin. Super-convergence: Very fast training of neural networks using large learning rates. In *Artificial intelligence and machine learning for multi-domain operations applications*, pages 369–386. SPIE, 2019.
- [49] Dominic Tarr, Erick Lavoie, Aljoscha Meyer, and Christian Tschudin. Secure Scuttlebutt: An Identity-Centric Protocol for Subjective and Decentralized Applications. In *ACM Conference on Information-Centric Networking*, pages 1–11, New York, NY, USA, 2019. Association for Computing Machinery.
- [50] Andrew Tridgell, Paul Mackerras, et al. rsync. <https://github.com/RsyncProject/rsync>, 2024. Accessed: 2024-08-23.
- [51] Kang Yu, Guoxin Tang, Wen Chen, Shanshan Hu, Yanzhou Li, and Haibo Gong. MobileNet-YOLO v5s: An Improved Lightweight Method for Real-Time Detection of Sugarcane Stem Nodes in Complex Natural Environments. *IEEE Access*, 11:104070–104083, 2023.